



Anatomical study of the scleral ring and eyeball of the long-eared owl (*Asio otus*) with anatomical methods and diagnostic imaging techniques

Omid Zehtabvar¹  | Majid Masoudifard²  | Okan Ekim³ | Faezeh Ghorbani⁵ | Somaye Davudypoor⁴ | Iman Memarian⁶ | Paniz Zarghami Dastjerdi⁵

¹Anatomy Sector, Department of Basic Sciences, Faculty of Veterinary Medicine, University of Tehran, Tehran, Iran

²Department of Surgery and Radiology, Faculty of Veterinary Medicine, University of Tehran, Tehran, Iran

³Department of Anatomy, Faculty of Veterinary Medicine, Ankara University, Ankara, Turkey

⁴Veterinary Radiologist, DVM, DVSc, Graduated from Faculty of Veterinary Medicine, University of Tehran, Tehran, Iran

⁵Graduated DVM Student, Faculty of Veterinary Medicine, University of Tehran, Tehran, Iran

⁶FPWC (Foundation for the Preservation of Wildlife Cultural Assets), IAR (International Animal Rescue), Felid Tag, Deer Tag, Persian Leopard and Cat Specialist Group (IUCN) Veterin Advisor, Yerevan, Armenia

Correspondence

Omid Zehtabvar, Department of Basic Sciences, Faculty of Veterinary Medicine, Anatomy Sector, University of Tehran, Tehran, Iran.
Email: ozehtabvar@ut.ac.ir

[Correction added on 26 May 2022, after first online publication: Faezeh Ghorbani's affiliation and affiliation 6 were corrected.]

Abstract

Background: The scleral ring in birds consists of ossicles that are fixed as small plates by cartilage joints and have no articulation to other parts of the skeleton.

Objective: Due to inadequate examination of the scleral ring anatomy and its specific form in owls, this study aimed to investigate the exact structure of the scleral ring and some morphometric characteristics of the eyeball in a long-eared owl (*Asio otus*).

Methods: The eyes of 20 alive and 10 dead male and female owls were examined. In addition to common anatomical methods, computed tomography scans and radiographic and ultrasonographic imaging techniques were used in this study.

Results: The structure consisted of 15 ossicles. In the ventral part of the ring, these tubercles were observed in the scleral rings of all owls; in each ring, there were four bones with these tubercles. Additionally, there was no significant difference between the left and right eye parameters. Most ocular parameters in female owls were larger than those in males, but in the case of some parameters, such as optic nerve length and optic nerve sheath diameter, this difference was not observed.

Conclusions: According to this study, the scleral ring in the *Asio otus* has anterior and posterior parts, and the lens is in the immediate vicinity of the anterior part. The right and left scleral rings and eyeballs are bilaterally symmetrical in terms of the shape, size, and number of ossicles that form the ring.

KEYWORDS

computed tomographic scan, CT anatomy, long-eared owl, scleral ring

1 | INTRODUCTION

The eyeball in birds closely resembles that of mammals. Its size, relative to the head size, is larger than the globe size in mammals (King and Mclelland, 1984). The overall shape is generally spheroid; however,

there are some controversies in different species, especially in the front part of the globe. The globe occupies the greatest space of orbit and is less mobile than the mammal's globe (Dyce et al., 2009). In the majority of bird species, the total weight of the eyes is greater than the weight of the brain (King and Mclelland, 1984).

This is an open access article under the terms of the [Creative Commons Attribution-NonCommercial](https://creativecommons.org/licenses/by-nc/4.0/) License, which permits use, distribution and reproduction in any medium, provided the original work is properly cited and is not used for commercial purposes.

© 2022 The Authors. *Veterinary Medicine and Science* published by John Wiley & Sons Ltd.

The diameter of the cornea is small in the avian eye and the cornea is protuberant, although the diameter of the globe is large (Dyce et al., 2009). The cornea is broader and more arched in owls and eagles (King and McLelland, 1984). The sclera forms the outer layer of the eye together with the cornea and has a solid structure that resists internal and external pressure and maintains the overall shape of the eye globe (King and McLelland, 1984; O'Malley, 2005).

The sclera is strengthened by globular cartilage, which, with aging, is sometimes transformed into an osseous structure (Dyce et al., 2009). The scleral ring in birds consists of ossicles that are fixed as small plates by cartilage joints and have no articulation to other parts of the skeleton (King and McLelland, 1984). It creates an intermediate region in the globe between the anterior part where the cornea is located and the posterior part of the globe, in which sclera forms a considerable volume. The intermediate part is oblong in a variety of owls and forms a stretched appearance for the front part of the globe. In general, it is stated that the owl's eyes are tubular shaped (King and McLelland, 1984; König et al., 2016). Large rings belong to animals that move very fast. Tubular scleral rings are a feature of the eye in owls and birds of prey. These birds move fast and have high visual acuity; in both cases, the specific structure of the ring is important. The ossicles that make up the ring are related to the length of the eye in the birds. This feature is especially present in owls. In the owls, the length of the ossicle can be twice as wide. Tubular scleral rings are more common in fast flying and aquatic birds. The largest ossicles are found in owls. The numbering of the ossicles starts from the ventral and continues in a mediolateral direction inclined towards the medial (nasal to temporal area). Ossicles that change coverage rhythm are called excellent ossicles. These ossicles are of two types, plus and minus. If both sides of an ossicle overlap their pre- and postossicles, it is called plus. If both sides of an ossicle are overlapped by the pre- and postossicles, it is called minus. If one side of the ossicle overlaps and the other side overlaps, this ossicle is called interlocked or imbricated. In birds, the scleral ring is divided into two types (A and B) based on the number of excellent ossicles. Type A has four excellent ossicles and type B has two excellent ossicles. Type B is found in owls and birds of prey. It has been pointed out that these features may differ in different species. It is noted that the number of ossicles in a bird's right and left rings may vary (Fischer and Schoenemann, 2019). Phylogenetic data based on scleral ring structure were not found to compare owl species. Regarding the function of the scleral ring, its role in accommodation is mentioned, the specific structure of this ring is probably related to this function in birds of prey and owls that have accurate vision and high flight speed (Franz-Odenaal, 2020). The general structure of the scleral ring in owls is the same, and the morphological and functional differences of the ring between different types of owls are not mentioned. One of the cases in which morphological differences are noted in owls is scleral sesamoid bone, which is a small structure next to the ring that has different shapes (Franz-Odenaal, 2020). In some cases, such as the Stygian owl (*Asio stygius*), this structure is a small bone that sits separately next to the scleral ring, and in others, such as the burrowing owl (*Speotyto cunicularia*), this structure is reported as a tubercle on the scleral ring. It is mentioned that the form of the eye does not seem to be fundamentally impor-

tant for nocturnal vision (Mahecha and Oliveira, 1998). Lisney et al. studied eye shape and retinal topography in owls. The results of their study provide evidence of interspecific variation in eye shape and retinal topography in owls. This variation is associated with different activity patterns and habitat preferences as opposed to phylogenetic relationships between species, as reflected by the clustering of species on the basis of similarities in eye shape and retinal topography. They did not study the structure of the scleral ring, scleral sesamoid, or the volume of the various sections (Lisney et al., 2012). In the general examination of raptors, eye examination is very important because a high prevalence of up to 50% of ocular disease can be found in free-living raptors. The most common ailments found in raptors are retinal degeneration, corneal lesions, retinal dysplasia, cataracts, glaucoma, ciliary body malformations, and traumatic uveitis (Gumpenberger and Kolm, 2006). As mentioned, Hassan et al. also noted that there are a few studies about radiography of the head or, more specifically, about the eyes of birds (Hwang et al., 2021). There are few studies related to the anatomy and ultrasonography of raptor's eyes. Recently, ultrasonography has become a routine procedure for veterinary ophthalmology. There is variation among the anatomy of birds, so it is impossible to use the same ultrasonographic and biometric measurements for every species (Hwang et al., 2021). Hwang et al. noted that information and measurements for both eyes were highly valuable for diagnosing the affected eyes for all species (Hwang et al., 2021).

Similar to birds, scleral rings are also found in various reptile species (King and McLelland, 1984). In the bird's sclera, there are scleral rings along the hyaline cartilage layer. Following are the two main functions assumed for this bony structure: it prevents the deformation of the globe during flight or diving, helps the ciliary muscles to act, and plays a critical role in eye accommodation. The specific functions of each ossicle forming this structure, however, are still under discussion (Franz-Odenaal, 2020; King and McLelland, 1984). This potential has not yet been addressed in all animal species possessing this structure (Lima et al., 2009). A variety of morphologies, numbers, and patterns of scleral ossicles can be observed in different groups of animals. In many birds, the ossicles are quadrilateral, while they are concave and stretched in others. In birds, 10-18 ossicles are involved in the formation of each ring (Dyce et al., 2009). The number of ossicles is higher in reptiles than in birds (Franz-Odenaal, 2006a, 2008a). The size of these ossicles is relatively large in owls (O'Malley, 2005). The scleral ring exists in many reptiles (other than crocodiles and snakes) as well as dinosaurs (Franz-Odenaal 2006a). The exact form of ossicles has not been properly documented in many animals. In a study conducted in 2008, it was concluded that these ossicles were dermal bones (Franz-Odenaal, 2008b).

Visual acuity is quite high in owls, and accordingly, their eye structure is of great importance. Long-eared owl (*Asio otus*) is one of the owl species in Iran. This species can also be found in Europe and America (Jobling, 2010). Diagnostic imaging techniques (Radiography, CT-Scan, MRI, Ultrasonography,...) are one of the best methods, not only for veterinary clinics to make diagnoses but also for anatomical studies. Various anatomists often use these techniques in their studies. The most prominent advantage of these techniques is that anatomical structures

can be investigated in live animals. Diagnostic imaging techniques are very suitable for anatomical studies of the coelomic cavity organs of animals such as turtles that are difficult to access, and methods such as computed tomography (CT) scans have been used for these studies (Zehtabvar et al., 2014, 2015). In addition, other methods, such as ultrasonography, have been used to study the anatomy of the heart structure in sturgeons (Zehtabvar et al., 2018, 2019). Diagnostic imaging techniques are used in anatomical studies of the eyeball. Gumpenberger and Kolm in 2006 used ultrasonography and CT for anatomic and pathologic studies on the avian eye. However, the differences between males and females were not considered. In this study, the structure of the long-eared owl's (*Asio otus*) eyeball was also examined. However, no attention was given to the differences between males and females and the anatomical features of the scleral ring (Gumpenberger and Kolm, 2006). In another study, Magnetic resonance imaging (MRI) was used on the orbit of the screech owl (*Megascops asio* or *Otus asio*). In a study on the eyeballs of birds that used ultrasonography and CT scans for morphometric studies, the long-eared owl was also examined, but the anatomical features of the scleral rings were not examined. In this study, the eyeballs of male and female owls were not compared. Eyeball volume was not studied in the study by Gumpenberger and Kolm (Gumpenberger and Kolm, 2006).

Due to the lack of proper examination of the scleral ring structure and its specific shape in owls, this study was focused on the exact structure of the scleral rings in the *Asio otus*. In addition, the shape, number, and pattern of scleral ossicles were examined in *Asio otus*. Another purpose of this study was to compare the eye structure of male and female long-eared owls.

2 | MATERIALS AND METHODS

2.1 | Individuals

Ten adult male and 10 adult female long-eared owls (*Asio otus*) were included in this study (350 ± 20.98 g male owls, 421 ± 31.12 g female owls). It should be noted that these specimens were being treated for locomotor system problems in the veterinary clinic (referred to the zoo rehabilitation clinic and wildlife centre). The owls belonged to Tehran Province in Iran. No owls were euthanised for this study. As explained below, all owls were anaesthetised and regained consciousness after the study. For gross anatomical studies, 10 dead specimens referred to a zoo veterinarian were used (five adult male and five adult female owls).

2.2 | CT scanning

After the transfer of all of the owls to the radiology department of the Small Animal Hospital in the Faculty of Veterinary Medicine, the subjects were first anaesthetised using ketamine (10 mg/kg body weight, IM) and xylazine (2 mg/kg body weight, IM) (Carpenter and Marion, 2017). Afterwards, a CT scan was performed for all subjects. Owls were positioned in ventral recumbency and all scans were obtained on a two-

detector scanner (Siemens Somatom Spirit/Germany) vertical to the longitudinal axes of the animal.

The technical parameters for this imaging protocol were as follows: rotation time, 1 s; slice thickness, 1 mm; reconstruction interval, 0.5–1 mm; pitch, 1; X-ray tube potential, 120 kV; and X-ray tube current, 130 mAs.

For each segment, the convenient window width (WW) and window level (WL) were selected for the section, which is referred to in each of the CT scan images. The bone window was used to examine the images. Furthermore, 3D images were reconstructed using the Osseous-Shaded-vp pattern. Syngo MMWP VE40A software was used for 3D reconstruction of digital images.

2.3 | Ultrasonographic examination

For efficient cranial and ocular ultrasonography, the ultrasonography machine and Linear Multi-Frequency Probe were preferred (GE Voluson730, 3–11 MHz). Sagittal sonograms were taken from the eyes.

2.4 | Radiographic studies

Radiographic images were taken with a digital radiography system (Kodak Directview CR 850) after dorsoventral positioning of the birds. To provide an optimum imaging quality, technical parameters were selected as follows: 4 mAs and 45 Kvp.

2.5 | Gross anatomical studies

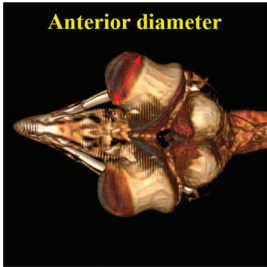
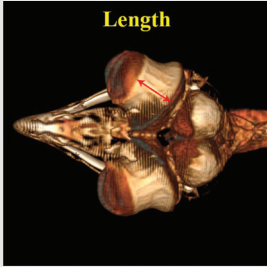
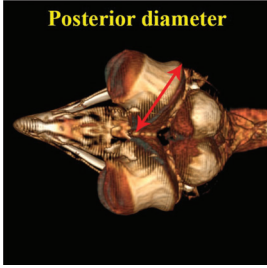
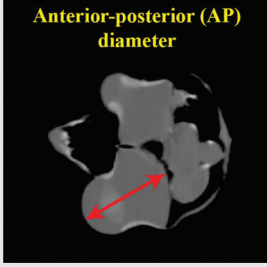
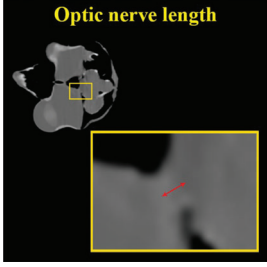
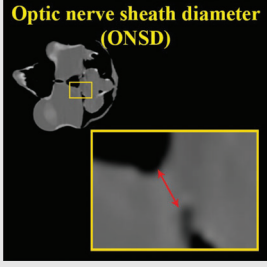
For this part of the study, the scleral rings of 10 dead birds (five adult male and five adult female owls that had died in the past 5 years and were brought to our department) were collected and isolated, and no bird was killed for this study. These dead birds were chosen by a chief veterinarian of the zoo.

Based on the information obtained in the previous stage and information available on other birds, anatomic analysis was performed. After separating the head of the specimens, the skin and unnecessary tissues were removed. All the osseous structures were macerated using the mealworm method (*Tenebrio molitor*) for 1 week (maintaining a temperature of 21°C and relative humidity of 70% to provide an optimum medium for insects). Once the cleaning of ossicles was completed, specimens were transferred to a stereo microscope, Olympus SZX12, equipped with the ASP-Cell Pad E digital camera for further investigation and acquisition.

2.6 | Morphometric studies

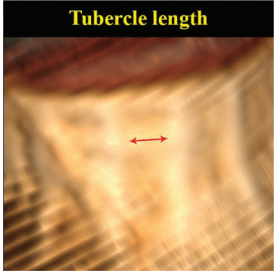
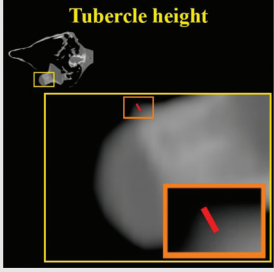
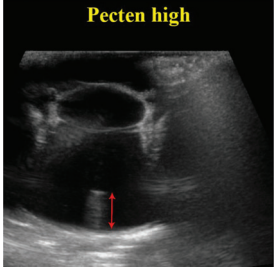
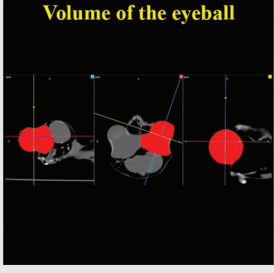
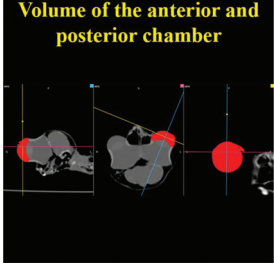
Morphometric mensuration from digital CT images was performed with Syngo MMWP VE40A software. The Hounsfield unit –120 to +1900 was selected for volumetric measurements in this software (Hounsfield unit for soft tissue and bone). In addition, some measurements were performed during ultrasonography. Table 1 shows the method of measurement.

TABLE 1 Morphometric parameters of the vertebral column. The measurement of the parameters (red line) is shown and the verticality of the image was adjusted for each parameter individually

Parameter	Measurements were taken at:	Description	Visual description
Anterior diameter (scleral ring)	3D CT scan images	Transverse diameter of the anterior part of the scleral ring was measured, the maximum distance was measured	
Length (scleral ring)	3D CT scan images	Horizontal distance between the anterior and posterior border of the scleral ring was measured, the maximum distance was measured	
Posterior diameter (scleral ring)	3D CT scan images	Transverse diameter of the posterior part of the scleral ring was measured, the maximum distance was measured	
Anterior-posterior (AP) diameter (eyeball)	2D Coronal CT scan images	Horizontal distance between the anterior and posterior border of the eyeball was measured, the maximum distance was measured	
Optic nerve length	2D Coronal CT scan images	The optic nerve was detected at the caudomedial position of the eyeball and its length was measured	
Optic nerve sheath diameter (ONSD)	2D Coronal CT scan images	The optic nerve was detected at the caudomedial position of the eyeball and its sheath diameter was measured	

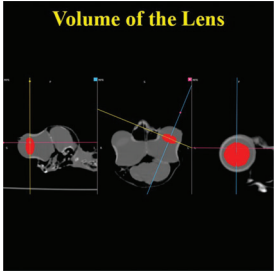
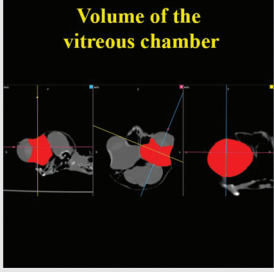
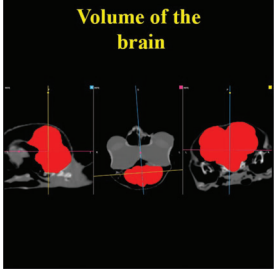
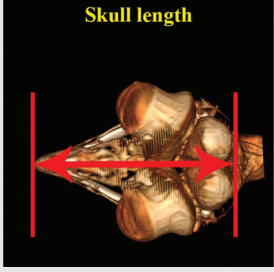
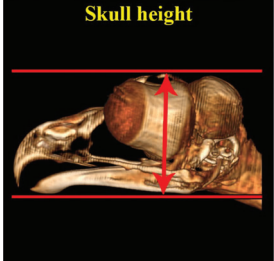
(Continues)

TABLE 1 (Continued)

Parameter	Measurements were taken at:	Description	Visual description
Tubercle length	3D CT scan images	The location of the tubercles was determined in the image and measured in fully vertical image mode; The verticality of the image was adjusted for each tubercle individually. For a better view of tubercles, you can refer to Figure 8c	
Tubercle height	2D Coronal CT scan images	The location of the tubercles was determined in the image and measured in fully vertical image mode; The verticality of the image was adjusted for each tubercle individually. For a better view of tubercles, you can refer to Figure 8c	
Pecten height	Sagittal ultrasonogram	The location of the pecten was determined in the image and measured in fully vertical image mode	
Volume of the eyeball	2D coronal, sagittal, and transverse CT scan images	In the dedicated section of measuring the volume of Syngo MMWP VE40A software, in all sections where the eyeball was identified, the structure range was specified in the transverse, coronal, and sagittal views, and finally, the software analysed these ranges in all sections and the volume was reported	
Volume of the anterior and posterior chamber	2D coronal, sagittal, and transverse CT scan images	In the dedicated section of measuring the volume of Syngo MMWP VE40A software, in all sections where the anterior and posterior chamber was identified, the structure range was specified in the transverse, coronal, and sagittal views, and finally, the software analysed these ranges in all sections and the volume was reported	

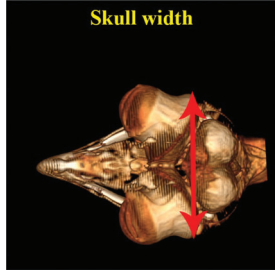
(Continues)

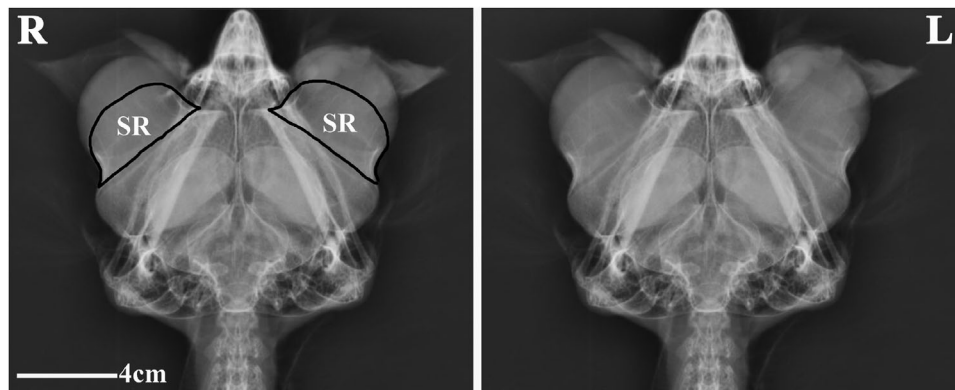
TABLE 1 (Continued)

Parameter	Measurements were taken at:	Description	Visual description
Volume of the Lens	2D coronal, sagittal, and transverse CT scan images	In the dedicated section of measuring the volume of Syngo MMWP VE40A software, in all sections where the lens was identified, the structure range was specified in the transverse, coronal, and sagittal views, and finally, the software analysed these ranges in all sections and the volume was reported	
Volume of the vitreous chamber	2D coronal, sagittal, and transverse CT scan images	In the dedicated section of measuring the volume of Syngo MMWP VE40A software, in all sections where the vitreous chamber was identified, the structure range was specified in the transverse, coronal and sagittal views, and finally, the software analysed these ranges in all sections and the volume was reported	
Volume of the brain	2D coronal, sagittal, and transverse CT Scan images	In the dedicated section of measuring the volume of Syngo MMWP VE40A software, in all sections where the brain was identified, the structure range was specified in the transverse, coronal, and sagittal views, and finally, the software analysed these ranges in all sections and the volume was reported	
Skull length	3D CT scan images	Horizontal distance between the anterior and posterior border of the skull was measured, the maximum distance was measured	
Skull height	3D CT scan images	Horizontal distance between the dorsal and ventral border of the eyeball was measured, the maximum distance was measured	

(Continues)

TABLE 1 (Continued)

Parameter	Measurements were taken at:	Description	Visual description
Skull width	3D CT scan images	Horizontal distance between the right and left border of the eyeball was measured, the maximum distance was measured	

**FIGURE 1** Dorsoventral radiograph of a long-eared owl (*Asio otus*) head. SR, scleral ring

Parameters of the right and left eye balls were compared by running a paired sample *t* test in SPSS software version 16 ($p > 0.05$).

3 | RESULTS

3.1 | Morphological (anatomical) results

As a general morphology, the scleral rings of the owls were semihyperbolic or in volcanic mountain form (Figures 1, 2, 4, and 7). There were two lateral and medial poles on the lateral and medial sides of the ring base (Figure 7). The base of this structure had two different diameters: a small diameter extended along an almost horizontal direction and the large diameter was almost vertical. The large diameter was placed between the two lateral and medial poles and the small diameter was approximately perpendicular (Figure 7). The medial wall of the ring was shorter than its lateral wall. The semihyperbolic structure of the scleral ring had two edges, anterior and posterior, and the circumference of the posterior edge was larger than that of the anterior edge. The posterior edge was the same as the base of the ring, which was oval. The anterior edge was almost circular. While the anterior edge was fairly smooth, the posterior edge was quite dentate (Figure 8). No connection or articulation was observed between the bone ring segments and skull bone structures. In general, it can be stated that this bone ring had

a tubular-shaped anterior section and a posterior funnel-shaped section (Figure 7). The overall structure of the bone ring, as well as the discussed features, were well observed in the two-dimensional (2D) transverse CT scan images and its sagittal and three-dimensional (3D) reconstructed images (Figures 1, 2, and 4). Since the images were prepared when the animals were alive and the soft tissues were evident in the images, the proximity of the lens to the anterior tubular part of the scleral ring was clear (Figure 2). In the 2D transverse and sagittal CT scan images, the adjacency of the lens with the anterior tubular part of the bone ring was noticed (Figure 3). In radiographs, the overall described structure of the ring and its placement in the skull were clearly identified (Figure 1). In ultrasonograms of the eye, an acoustic shadow was observed in the posterior regions of the bone ring (Figure 5).

The structure of the scleral right and left rings in all subjects and specimens consisted of 15 ossicles (Figure 7). The segments were quadrilateral and had rectangular shapes. The inner surface of these segments protruded inside with a prominent convexity (Figures 6 and 7) and the outer surface was indented (Figure 6). The long borders of segments were fused to form the body of the scleral ring, and the short sides took part in the formation of the anterior and posterior border of the scleral rings (Figure 7). Each of the bone segments was wider in the centre than at the edges (Figure 7). At the long borders of each segment, there was a specific surface that provides a binding area for the long border of an adjacent segment. At these surfaces, the

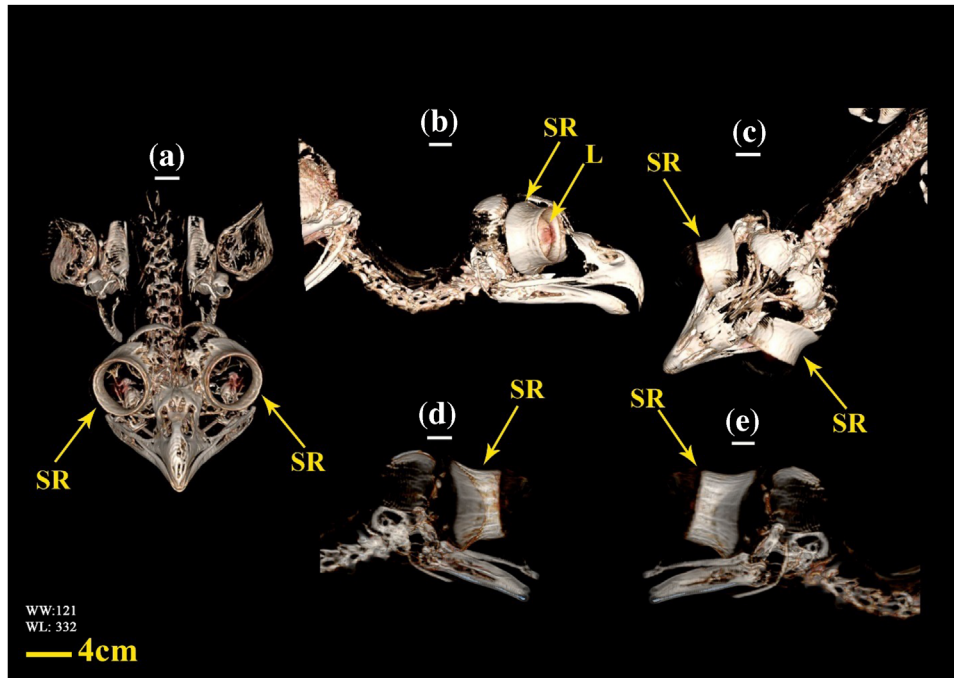


FIGURE 2 Three-dimensional (3D) reconstruction images (osseous-shaded-vp) of the long-eared owl (*Asio otus*), showing bones of the head and neck, (a) Anterior view, (b) Lateral view, (c) Dorsal view, (d) Left sagittal section view, (e) Right sagittal section view. L, lens; SR, scleral ring

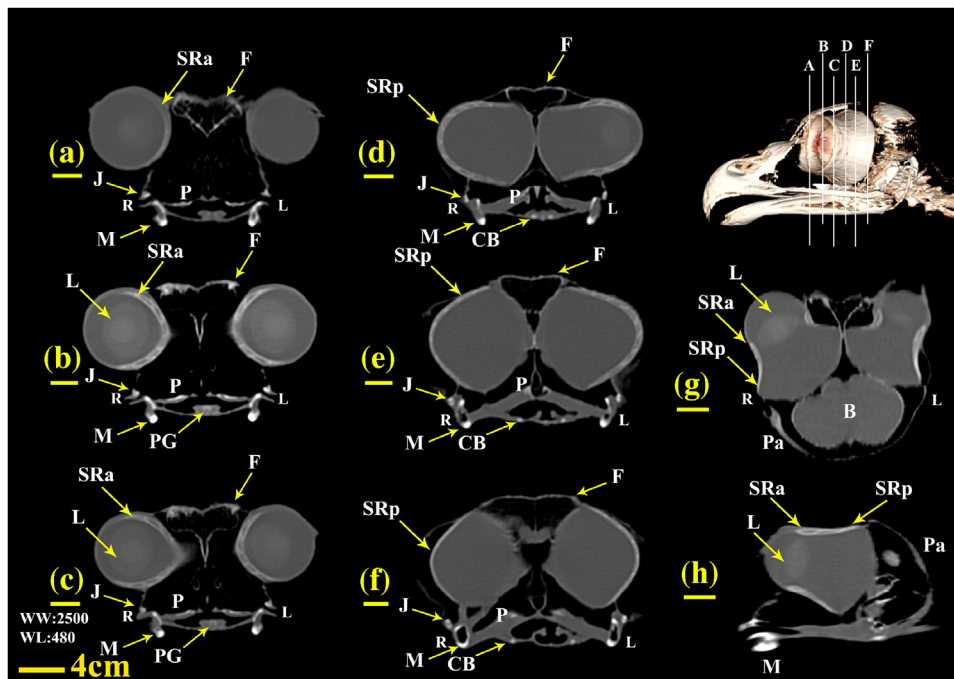


FIGURE 3 Computed tomography images (bone window) of the long-eared owl (*Asio otus*), (a-f) transverse planes, (g) dorsal plane, (h) left sagittal plane. Right and left are marked with R and L in each image. B, brain; CB, ceratobranchiale; F, frontal bone; J, jugal bone; L, lens; M, mandible; P, palatine bone; Pa, parietal bone; PG, paraglossum; SB, sesamoid bone of sclera; SRa, anterior part of the scleral ring; SRp, posterior part of the scleral ring

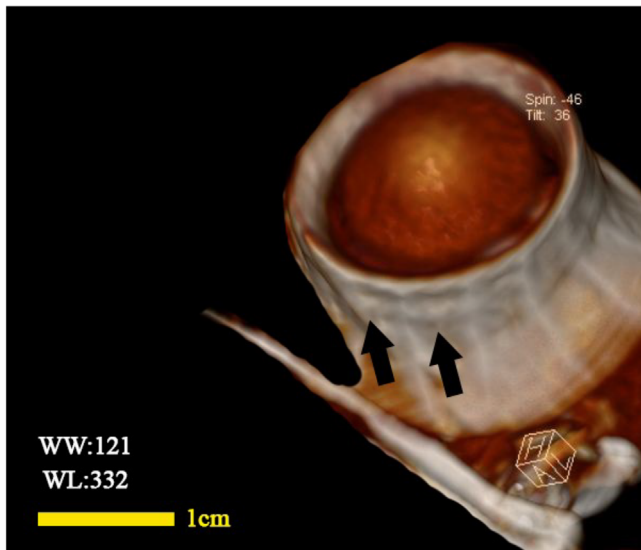


FIGURE 4 Three-dimensional (3D) reconstruction images (osseous-shaded-vp) of the long-eared owl (*Asio otus*), Medial view and tubercles are noted. For a better view of tubercles, you can refer to Figure 8c

bone was indented at a constant angle, and bone segments formed a ring-like structure (Figures 7 and 8). The border between the bone segments was also imaged in 2D and 3D CT scan images (Figures 2, 3, and 4). In radiographic images, the boundary between bone segments was partially observed (Figure 1). Of the 15 ossicles that make up the ring, two were excellent ossicles. The numbering of the ossicles is shown in

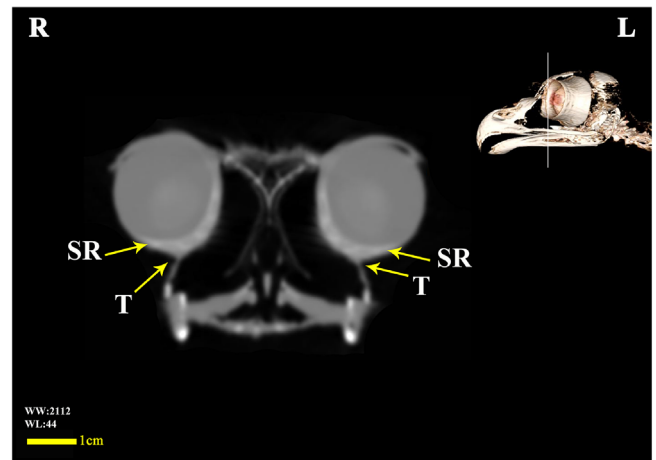


FIGURE 6 Transverse computed tomography image (bone window) of the long-eared owl (*Asio otus*). SR, scleral ring; T, tubercle

Figure 7. In this study, ossicle number one was plus and ossicle number six was minus (Figure 9).

In the ventral part of the ring, only in the four bone segments (ossicles), there were some small tubercles on the outer surface in all specimens, close to the anterior edge, which were not detected in other segments of these structures (Figure 8). These tubercles were well defined in stereomicroscopic images and observed in CT scan images (Figure 6) but not in radiographs. It should be noted that the CT scan image of Figure 6 was taken transversely from the owl's head and the scleral ring in the skull is almost oblique, so the structure of the tubercles seen in

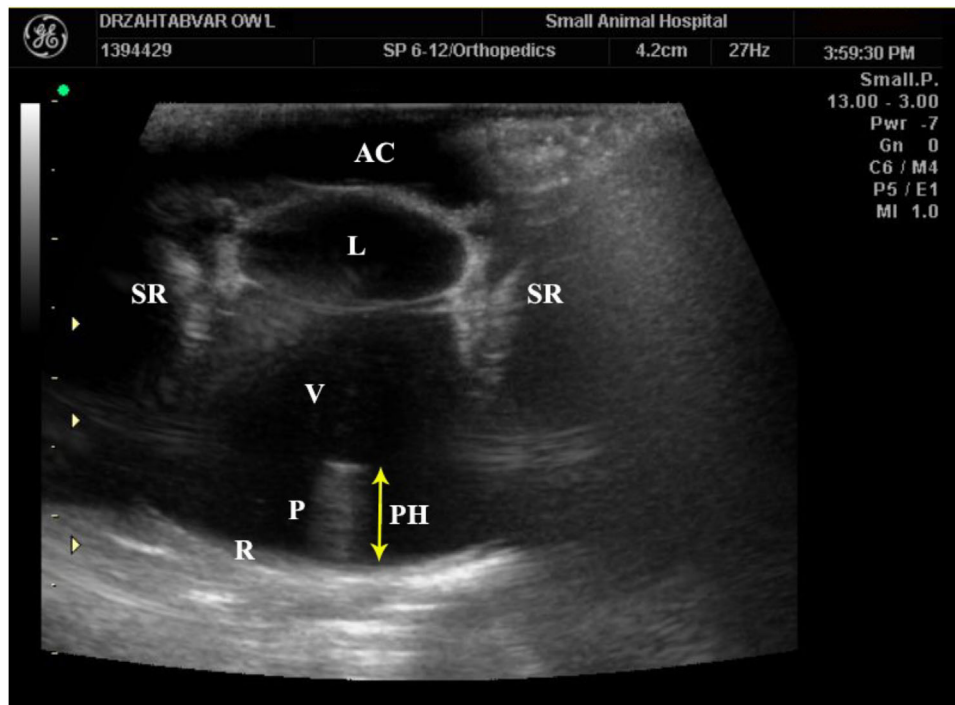


FIGURE 5 Sagittal ultrasonogram of the long-eared owl's (*Asio otus*) eye. AC, anterior and posterior chamber; L, lens; P, pecten; PH, pecten height; R, retina; SR, acoustic shadowing of the scleral ring; V, vitreous chamber

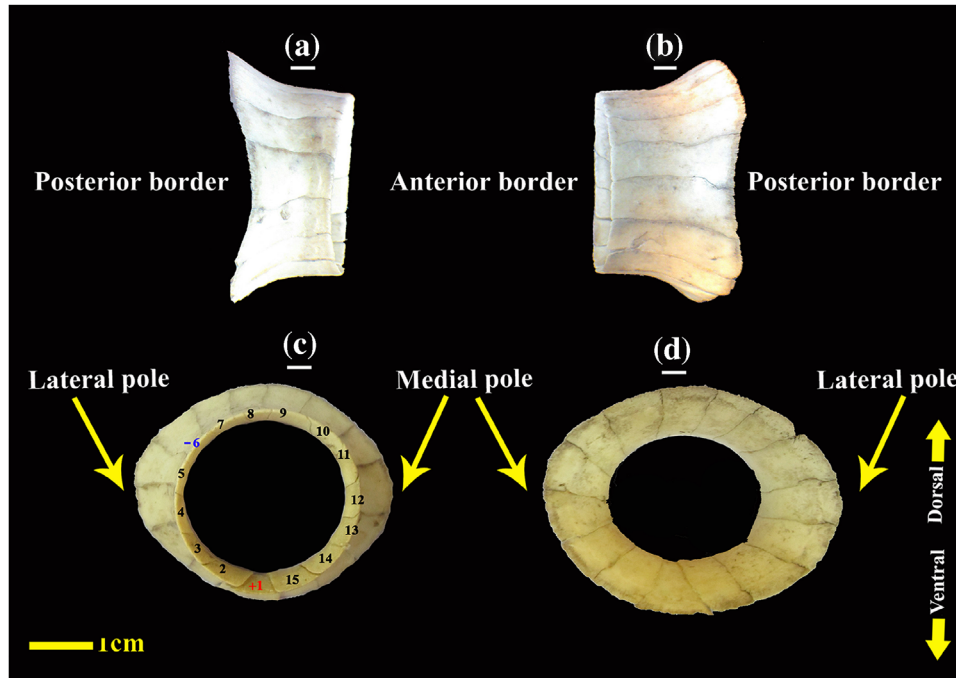


FIGURE 7 Scleral ring of the long-eared owl (*Asio otus*), (a) Lateral view, (b) medial view, (c) anterior view, numbering is shown, plus and minus excellent ossicles are shown (+1 and -6) (d) Caudal view

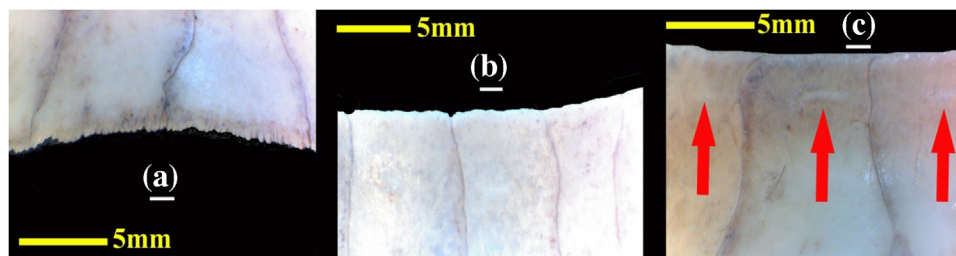


FIGURE 8 Scleral ring of the long-eared owl (*Asio otus*), (a) posterior border, (b) anterior border, (c) tubercles

Figure 8 is obliquely in Figure 6, so they have a different view. In addition, one of the tubercles is shown in Figure 6. Of the four tubercles, the tubercle was larger on the fourteenth ossicle. The length and height of this tubercle were measured in each eye (Table 2). These four tubercles were found in ossicles 12-15.

3.2 | Morphometric results

Measurements of tubercles were performed on the tubercle of the fourteenth ossicle, which was larger and more distinct than the others. The difference in tubercle length and height between right and left eyes was not statistically significant ($p > 0.05$) (Table 2). The difference in tubercle length and width between males and females was statistically significant. Therefore, it can be said that this tubercle was larger in females ($p < 0.05$) (Table 2).

There was no significant difference between the left- and right-eye morphometric parameters in the male and female birds ($p > 0.05$)

(Tables 2 and 3). There was a significant difference between male and female owls and all parameters of female owls were larger than those of male owls ($p < 0.05$) (Tables 2 and 3). Therefore, female owls had larger eyeballs than males. Females also had longer and wider optic nerves.

There was a significant difference between the length, height, and width of the skull of the male and female owls. Female skulls were longer, wider, and taller than males ($p < 0.05$) (Table 4).

There was a significant difference between the volume of the eyeballs and brain, and the eyeballs had a larger volume in the male and female owls ($p < 0.05$) (Table 2). In the right and left eyes of male and female owls, the difference between the anterior and posterior chambers and vitreous chamber volume was statistically significant. In addition, the difference in lens volume with the vitreous chamber was significant ($p < 0.05$) (Table 3). However, the difference between the volume of the lens and the anterior and posterior chambers was not significant ($p > 0.05$) (Table 3). Based on these statistical results, it can be said that the volumes of the anterior and posterior chambers and the lens are equal and that the vitreous chamber has a larger volume.

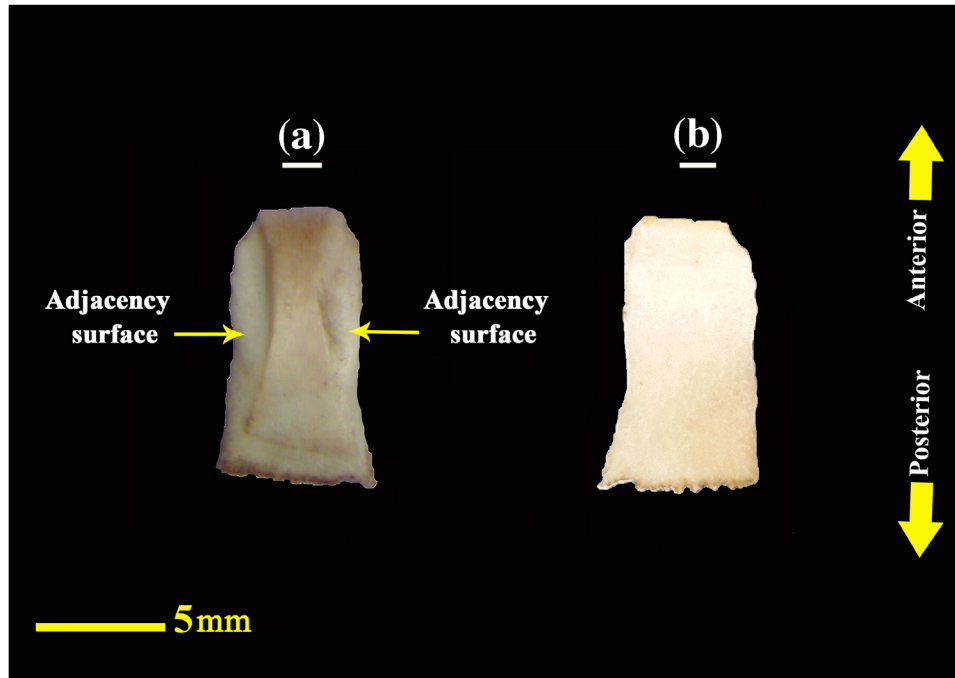


FIGURE 9 Scleral ring plus excellent ossicle (ossicle number one) of the long-eared owl (*Asio otus*), (a) inner surface, (b) outer surface

TABLE 2 Measured parameters of the scleral ring and eyeballs of the male and female long-eared owl (*Asio otus*) (mm)

Parameters	Male owls		Female owls	
	Mean \pm SD (Right eye)	Mean \pm SD (Left eye)	Mean \pm SD (Right eye)	Mean \pm SD (Left eye)
Anterior diameter (scleral ring)	24.50 \pm 1.18	24.33 \pm 1.22	26.82 \pm 1.22 ^a	27.03 \pm 1.31 ^a
Length (scleral ring)	14.56 \pm 1.31	14.44 \pm 1.24	17.06 \pm 1.43 ^a	16.64 \pm 1.14 ^a
Posterior diameter (scleral ring)	36.85 \pm 0.39	37.05 \pm 1.21	39.15 \pm 1.44 ^a	38.81 \pm 1.19 ^a
Anterior-posterior (AP) diameter (eyeball)	20.89 \pm 1.42	21.09 \pm 1.32	21.99 \pm 1.31 ^a	22.09 \pm 1.23 ^a
Optic nerve length	4.12 \pm 0.44	4.27 \pm 0.33	3.92 \pm 0.21	4.11 \pm 0.41
Optic nerve sheath diameter (ONSD)	3.92 \pm 0.31	3.87 \pm 0.42	4.02 \pm 0.33	4.11 \pm 0.12
Tubercle length	3.56 \pm 0.31	3.40 \pm 0.44	4.44 \pm 0.11 ^a	4.20 \pm 0.21 ^a
Tubercle height	0.26 \pm 0.14	0.31 \pm 0.11	0.37 \pm 0.09 ^a	0.39 \pm 0.11 ^a
Pecten height	6.42 \pm 0.23	6.65 \pm 0.23	6.66 \pm 0.12	6.45 \pm 0.13

^aEach column represents a significant difference between male and female parameters ($p < 0.05$). In this table, statistical analysis of the parameters recorded in different columns has been done and a comparison between rows has not been done, in addition, the comparison of right and left in one sex with itself has not been done.

TABLE 3 Measured volumes of the eyeballs and brain of the male and female long-eared owl (*Asio otus*) (cm³)

Parameters	Male owls		Female owls	
	Mean \pm SD (Right eye)	Mean \pm SD (Left eye)	Mean \pm SD (Right eye)	Mean \pm SD (Left eye)
Volume of the eye ball	25.26 \pm 1.31	25.77 \pm 1.22	29.16 \pm 1.22 ^a	29.27 \pm 1.32 ^a
Volume of the anterior and posterior chamber	4.21 \pm 0.23	4.32 \pm 0.32	5.42 \pm 0.44 ^a	5.61 \pm 0.32 ^a
Volume of the Lens	4.01 \pm 0.33	4.21 \pm 0.12	5.71 \pm 0.23 ^a	5.63 \pm 0.12 ^a
Volume of the vitreous chamber	16.72 \pm 1.44	17.21 \pm 1.01	17.95 \pm 1.54 ^a	18.12 \pm 1.01 ^a
Volume of the brain	21.03 \pm 1.15		25.22 \pm 1.45 ^a	

^aEach column represents a significant difference between male and female parameters ($p < 0.05$). In this table, statistical analysis of the parameters recorded in different columns has been done and a comparison between rows has not been done, in addition, the comparison of right and left in one sex with itself has not been done.

TABLE 4 Measured parameters of the skull of the male and female long-eared owl (*Asio otus*) (mm)

Parameters	Male owls	Female owls
	Mean ± SD	Mean ± SD
Skull length	54.65 ± 1.29	56.23 ± 1.33 ^a
Skull height	40.38 ± 1.39	43.08 ± 1.21 ^a
Skull width	66.69 ± 1.47	68.51 ± 1.35 ^a

^aEach column represents a significant difference between male and female parameters ($p < 0.05$). In this table, statistical analysis of the parameters recorded in different columns has been done and a comparison between rows has not been done, in addition, the comparison of right and left in one sex with itself has not been done.

In the female and male owls, the difference in brain volume with the right and left eyes was statistically significant ($p < 0.05$) (Table 3). Based on these statistical results, it can be said that in male and female owls, the eyes have a larger volume of the brain. The difference in height between right and left pecten in both sexes was not statistically significant ($p > 0.05$) (Table 2). The difference in pecten height between males and females was not statistically significant ($p > 0.05$) (Table 2). The difference in optic nerve length and optic nerve sheath diameter (ONSD) between males and females was not statistically significant ($p > 0.05$) (Table 2).

4 | DISCUSSION

The general form of the scleral ring and its constituent segments is one of the remarkable specifications that can be used for classification or taxonomy of species. Regarding *Athene cunicularia*, the structure reported resembles the one observed for the *Asio otus* in this study (Lima et al. 2009). It has been documented that the ellipsoidal shape of the globe has an impact on the shape of the ossicles in *Strigiformes*, *Falconiformes* and aquatic birds, which ultimately makes the globe tubular, and such a shape of the eye does not change against the pressure of air and water (King and McLelland, 1984). It should also be pointed out that the presence of this bone structure in various forms that could prevent the passage of ultrasound waves should be considered in performing eye ultrasonography.

There are reports on fractures of this bone structure in a number of cases because of head injury. Denise et al. reported a fracture in the scleral ring of a *Buteo jamaicensis* using radiography (Denise et al., 1988). In 1988, scientists examined the structure of the scleral ring and its phylogenetic connections in *Ophisthocomus hoazin* (Queiroz and Good, 1988). According to Franz's studies in 2008, it can be claimed that Teleostei can have two shapes (namely, rounded and stretched arched) with respect to the scleral ossicles (Franz-Odendaal, 2008a; Jobling, 2010). In a study on the phylogeny of the scleral ring in fish and birds, it was found that the cartilaginous structures that will turn into the ossicles in this structure originate from scleral cartilage, although they are dermal bones in birds (Lima et al., 2009). It should be noted that Franz-Odendaal et al. in 2007 were the first to study the devel-

opmental and morphological variation in the teleost craniofacial skeleton. Franz-Odendaal et al. pointed out that scleral ossicles in teleosts may not be homologous to those in other vertebrates, such as reptiles. (Franz-Odendaal et al., 2007). Franz-Odendaal and Hall (2006b) also noted that homology cannot be assumed for scleral skeletal elements, although they share the same name, scleral ossicles.

Franz-Odendaal researched the morphology of cartilaginous structures that turn into ossicles and ossification with the growth stages for chickens (Franz-Odendaal, 2008b). In 2009, the structure of the ossicles was examined in Brazilian birds. It was noted in this study that there are 17 ossicles in *Athene cunicularia*'s eye (Lima et al., 2009); however, there were 15 ossicles observed in the case of the *Asio otus*. In the current study, it was revealed that the medial ring wall in the *Asio otus* is longer than the lateral wall. Furthermore, the anterior border was smoother than the posterior border. Needless to say, the anterior border faces the cornea and the posterior border is in front of the sclera. Franz-Odendaal and Krings in 2019 noted a heterochronic shift in the timing of scleral cartilage development and ossicle mineralisation (but not induction) to later in development compared to in chickens and suggested that the scleral ossicles are likely functionally important bones for vision in owls and possibly other altricial species.

In 1998, some studies indicated that the sclerotic ring in owls and some other birds possesses a bone segment that was not regarded or described in previous studies. The bone is located on the pyramidal muscle tendon and has a sulcus to pass it. It has been reported that this structure prevents the splitting of the muscle from the sclera during contraction and tendon deviation during muscle function. Concerning the pyramidal muscle, it is linked to the nictitating membrane or third eyelid in the owls, which is at the upper edge of the globe. Mahecha, in his study, stated scleral sesamoid bone for this structure (Mahecha and Oliveira, 1998). In the present study, there was no osseous structure separated from the scleral ring, even though there were small bony tubercles at the outer surface of the ring, near the anterior edge of four ossicles, constituents of the ring. Due to failure to notice a separate bone structure as scleral sesamoid bone, these structures seem to be their equivalent and perform the same function. It should be highlighted that these structures have not been discussed or even reported in previous studies conducted on the scleral ring. In the striped owl (*Asio clamator*), Rodarte-Almeida noted that one scleral sesamoid was located anteriorly and medially, close to the anterior margin of the scleral ossicle ring, a margin that corresponds to the region of the corneal limbus in the living being, and the scleral cartilaginous lamina was fixed to the posterior margin of the ossicle ring (Rodarte et al., 2013). In another study focused on Brazilian bird species, a scleral sesamoid bone was also mentioned in *Cariama cristata* (Lima et al., 2009). Mahecha noted that the specific structure of the scleral sesamoid bone was not observed in *Glaucidium brasilianum*; however, it is small and rounded in *Athene cunicularia*, stretched in *Bubo bubo*, and stretched and two-segmental in *Bubo virginianus*. Conversely, none of these forms was noticed in the species researched in this study. According to radiographs and 2D and 3D CT scan images, the probability of the presence of a bone and its being disregarded because of a

mistake in the bone isolation process is almost zero. Whether there was a structure in a size reported by Mahecha (approximately 3 mm), it would be visible in our CT scan images, which were prepared with a 1-mm slice thickness. With regard to *Athene cunicularia*, it seems possible that the bone structure of the scleral sesamoid bone was similar to the species examined in the current study (Mahecha and Oliveira, 1998). Based on information provided in other studies, the scleral ring in owls is type B. Fischer and Schoenemann pointed out that in this type of scleral ring, ossicle number one is plus excellent ossicles and bone number seven is minus excellent ossicles (Fischer and Schoenemann, 2019). As mentioned in the case of the *Asio otus*, ossicle number one is plus and ossicle number six is minus. In the article mentioned, the number of ossicles, such as *Asio otus*, was 15.

Based on the various shapes observed in this study and other studies in the case of owls, it seems that the bone structures associated with pyramidal muscle are in two forms: a bone structure separated from the scleral ring, which is called the scleral sesamoid bone, and a few prominences on the bone towards the pyramidal muscle. These structures can be called the scleral ring tubercle or scleral tubercle. Of course, the frequency of the tubercles in the scleral ring is greater than their frequency in scleral sesamoid bones. In all reported cases, there was one bone reported for each eye but four tubercles in the *Asio otus*. On the other hand, the height and length of these tubercles are less than those in the scleral sesamoid bones (Mahecha and Oliveira, 1998). Further research is suggested to be on *Athene cunicularia* to determine the types of structures relevant to the pyramidal muscle. Histologic studies on the scleral sesamoid bones have shown that this structure has a thin and modular cortex with a thin periosteum that is in contact with the periosteum of the bones forming the ring (O'Malley, 2005). According to the cases mentioned, it can be said that these tubercles are of two types; one type observed in some owls is that of a tubercle, a condition reported in *Asio clamator*. Of course, Rodarte-Almeida called this structure sesamoid, but according to the pictures presented in the article, this structure is tubercle-shaped (Rodarte et al., 2013). Another type of structure is one in which there are several tubercles on the ring, but these tubercles are smaller than the previous type. In this study, we observed this type in the case of *Asio otus*. Stygian owl (*Asio stygius*) is one of the owls that is close to our owl (*Asio otus*) in terms of scientific classification (taxonomy); both owls mentioned belong to the common genus *Asio*. However, in *Asio stygius*, there is a structure in the form of a sesamoid bone, while in *Asio otus*, there are several tubercles. Mahecha and Oliveira note that no cladistic analysis was presented for owls in the present study; also, we did not find complete information about this type of classification (Mahecha and Oliveira, 1998). Therefore, using information from scleral ring and scleral sesamoid bone morphological studies in owls to extract phylogenetic information and cladistic analysis can be suggested.

In the case of humans, a study noted that there are differences in the morphometric parameters of the right and left eyes, which causes asymmetry of the right and left eyeballs in humans. In this study, it is mentioned that there is an asymmetry in diameter but not in the case of eyeball volume. Except in some cases, the parameters measured in women's eyeballs are smaller than in men's eyeballs. One of these

parameters that is not different in the eyeballs of men and women is the volume (Murat et al., 2016).

Based on the results of this study in the *Asio otus*, it can be said that the sizes of different eye structures in females were larger than those in males. The same is true of skull measurements, and females had larger skulls. These differences in eye and skull size appear to be related to differences in body size and weight of male and female birds (O'Malley, 2005). It should be noted that no asymmetry was observed in the studied structures in the right and left eyes. The lack of difference in pecten height between male and female owls, despite the difference in eye size, seems to be a concern for future studies. The pigmented, highly vascular pecten arises from the retina at the ovoid exit point of the optic nerve and protrudes into the vitreous body. It is unique to the eye of birds. The function of the pecten remains unclear. The lack of pecten height difference between males and females may also cause differences in their vision. In a study on *Coturnix coturnix japonica*, this difference between males and females was not observed (Orhan et al., 2011). It is mentioned that pecten might play a role in thermoregulation and absorption of light (Orhan et al., 2011); no difference in pecten height between male and female birds despite the difference in volume and some other sizes of the eyeball can cause differences in vision between males and females. It is suggested that studies in this field be performed in the future. Hwang et al. noted that for birds of prey, ultrasound is one of the best ways to examine the eye, as it can be performed without anaesthesia (Hwang et al., 2021).

In the present study, CT allowed proper visualisation of the lens, anterior eye chamber, posterior eye chamber, cornea, scleral ring, ocular nerve, retrobulbar space, and whole skull except for examination. It should be noted that in CT, it was not possible to examine pecten separately from the vitreous chamber, which was eliminated by ultrasonography. This issue has been addressed in similar studies (Hwang et al., 2021). It should be noted here that the average height of the pecten in *Asio otus* is less than that of *Aegypius monachus* (11.47–13.50 mm) but is almost in the same range as that of *Asio clamator* (4.49–6.73 mm). Of course, the difference in body size of these birds should be noted.

According to the observations made in this study on the scleral ring in the *Asio otus*, it can be concluded that it has anterior and posterior parts. The anterior part is tubular with an almost circular cross-section and the posterior part is infundibular with an almost oval cross-section. The eye lens is in the immediate vicinity of the anterior part. In the ventral part of the scleral ring, there are some small tubercles on the outer surface of the rings. In the case of the right and left scleral rings, it can be said that in terms of the number of ossicles, the shape and size have a symmetrical structure. The eye and most of its related structures studied in this study were larger in females than in males, but in some cases, such as optic nerve length, optic nerve sheath diameter, and pecten height, no difference was observed. These cases and their effect on the visual status of males and females should be considered in future studies. In this owl, we observed several tubercles instead of the scleral sesamoid bone. These tubercles were described in terms of size, shape, and connections, and it was suggested that the term "scleral tubercle" be used instead of "scleral sesamoid" in this owl. Similar species will be found in other studies. Based on the results of this

article and other similar articles, scleral tubercles can be divided into two types, one type in which there is a large tubercle instead of the scleral sesamoid. The other type is that there are several small tubercles next to each other on the scleral ring. It should be noted that several small tubercles were observed in *Asio otus*.

One of the most important points in this study is that we did not euthanise any animal and all 20 of the samples were alive after our study. It can be asserted that diagnostic imaging techniques are very useful not only for avian clinics but also for anatomical studies focused on endangered or endemic species.

ACKNOWLEDGEMENT

The authors wish to express their appreciation to everyone who assisted in this study, especially the staff of the anatomy and radiology departments of the Faculty of Veterinary Medicine, University of Tehran.

CONFLICTS OF INTEREST

The authors declare that they have no conflicts of interest.

ETHICS STATEMENT

This study was a doctor of veterinary medicine thesis and all experimental procedures were approved by the Faculty of Veterinary Medicine, University of Tehran Local Ethics Committee (30704/6/5).

DATA AVAILABILITY STATEMENT

Data available on request from the authors.

PEER REVIEW

The peer review history for this article is available at <https://publons.com/publon/10.1002/vms3.823>

ORCID

Omid Zehtabvar  <https://orcid.org/0000-0002-4343-4453>

Majid Masoudifard  <https://orcid.org/0000-0001-9087-6919>

REFERENCES

- Carpenter, J. W., & Marion, C. (2017). *Exotic animal formulary* (5th ed.) Elsevier Science.
- Denise, M. L., Hathcock, J. T., Miller, W. W., & Di Pinto, M. N. (1988). Fractured scleral ossicles in a red tail hawk. *Veterinary Radiology and Ultrasound*, 29(209–212). <https://doi.org/10.1111/j.1740-8261.1988.tb01501.x>
- Dyce, K. M., Sack, W. O., & Wensing, C. J. G. (2009). *Textbook of veterinary anatomy* (4th ed.) Elsevier Science.
- Fischer, O., & Schoenemann, B. (2019). Why are bones in vertebrate eyes? Morphology, development and function of scleral ossicles in vertebrate eyes—A comparative study. *Anatomy and Physiological Studies*, 3(2), 1–26.
- Franz-Odendaal, T. A., & Hall, B. K. (2006b). Skeletal elements within teleost eyes and a discussion of their homology. *Journal of Morphology*, 267(11), 1326–1337. <https://doi.org/10.1002/jmor.10479>
- Franz-Odendaal, T. A., & Krings, M. (2019). A heterochronic shift in skeletal development in the barn owl (*Tyto furcata*): A description of the ocular skeleton and tubular eye shape formation. *Developmental Dynamics: An Official Publication of the American Association of Anatomists*, 248(8), 671–678. <https://doi.org/10.1002/dvdy.65>
- Franz-Odendaal, T. A., Ryan, K., & Hall, B. K. (2007). Developmental and morphological variation in the teleost craniofacial skeleton reveals an unusual mode of ossification. *Journal of Experimental Zoology. Part B, Molecular and Developmental Evolution*, 308(6), 709–721. <https://doi.org/10.1002/jez.b.21185>
- Franz-Odendaal, T. A. (2006). Intramembranous ossification of scleral ossicles in *chelydra serpentina*. *Zoology*, 109(1), 75–81. <https://doi.org/10.1016/j.zool.2005.10.001>
- Franz-Odendaal, T. A. (2008a). Scleral ossicles of teleostei: evolutionary and developmental trends. *Anatomical Record*, 291(22), 161–168. <https://doi.org/10.1002/ar.20639>
- Franz-Odendaal, T. A. (2008b). Toward understanding the development of scleral ossicles in the chicken, *gallus gallus*. *Developmental Dynamics*, 237(11), 3240–3251. <https://doi.org/10.1002/dvdy.21754>
- Franz-Odendaal, T. A. (2020). Skeletons of the eye: An evolutionary and developmental perspective. *Anatomical Record*, 303(1), 100–109. <https://doi.org/10.1002/ar.24043>
- Gumpenberger, M., & Kolm, G. (2006). Ultrasonographic and computed tomographic examinations of the avian eye: physiologic appearance, pathologic findings, and comparative biometric measurement. *Veterinary Radiology & Ultrasound*, 47, 492–502. <https://doi.org/10.1111/j.1740-8261.2006.00168.x>
- Hwang, J., Kang, S., Seok, S., Ahmed, S., Jeong, D. H., & Yeon, S. (2021). Imaging characteristics of the eyes of cinereous vulture (*Aegypius monachus*): morphology and comparative biometric measurement. *JVMS*, 83(8), 1330–1337. <https://doi.org/10.1292/jvms.21-0119>
- Jobling, J. A. (2010). *The helm dictionary of scientific bird names*. Christopher Helm.
- King, A. S., & Mclelland, J. (1984). *Birds their structure and function* (2nd ed.) Bailliere Tindall.
- König, H. E., Korbelt, R., & Liebich, H. G. (2016). *Avian anatomy*. 5M Publishing.
- Lima, F. C., Vieira, L. G., Santos, A. L. Q., Simone, S. B. S., Hirano, L. Q. L., Silva, J. M. M., & Romão, M. F. (2009). Anatomy of the scleral ossicles in Brazilian birds. *Brazilian Journal of Morphological Sciences*, 26, 165–169.
- Lisney, T. J., Iwaniuk, A. N., Bandet, M. V., & Wylie, D. R. (2012). Eye shape and retinal topography in owls (Aves: Strigiformes). *Brain Behavior and Evolution*, 79(4), 218–236. <https://doi.org/10.1159/000337760>
- Mahecha, G. A. B., & Oliveira, A. (1998). An additional bone in the sclera of the eyes of owls and the common potoo (*Nictibius griseus*) and its role in the contraction of the nictitating membrane. *Acta Anatomica*, 163(4), 201–211. <https://doi.org/10.1159/000046499>
- Murat, Ö. C., Ilker, Ö. I., Serifoğlu, I., Çağatay Büyüksal, M., & Barut, C. (2016). Evaluation of eyeball and orbit in relation to gender and age. *Craniofacial Surgery*, 27(8), 793–800. <https://doi.org/10.1097/scs.0000000000003133>
- O'Malley, B. (2005). *Clinical anatomy and physiology of exotic species*. Elsevier.
- Orhan, O., Ekim, O., & Bayraktaroglu, A. G. (2011). Morphological investigation of the pecten oculi in quail (*Coturnix coturnix japonica*). *Ankara Üniversitesi Veteriner Fakültesi Dergisi*, 58, 5–10.
- Queiroz, Q., & Good, D. A. (1988). The scleral ossicles of opisthocomus and their phylogenetic significance. *Ornithology*, 105, 29–35. <https://doi.org/10.1093/auk/105.1.29>
- Rodarte-Almeida, A. C. V., Machado, M., Baldotto, S. B., Leigue dos Santos, L., Lima, L., Lange, R. R., Froes, T. R., & Montiani-Ferreira, F. (2013). The eye of the striped owl: morphologic observations, biometric findings and reference values for selected ophthalmic diagnostics tests. *Pesquisa Veterinária Brasileira*, 33(10), 1275–1289.
- Zehtabvar, O., Tootian, Z., Vajhi, A. R., Shojaei, B., Rostami, A., Davudypoor, S., Sadeghinezhad, J., Ghaffari, H., & Memarian, I. (2014). Computed tomographic anatomy and topography of the lower respiratory system of the European pond turtle (*Emys orbicularis*). *Iranian Journal of Veterinary Surgery*, 9(2), 9–16.

- Zehtabvar, O., Vajhi, A. R., Tootian, Z., Masoudifard, M., & Davudypoor, S. (2019). Investigating the echocardiography and heart anatomy of immature beluga (*Huso huso*). *Iranian Journal of Veterinary Surgery*, 14(1), 44–53. <https://doi.org/10.22034/ivsa.2019.149748.1160>
- Zehtabvar, O., Vajhi, A. R., Tootian, Z., Masoudifard, M., Sadeghinezhad, J., & Davudypoor, S. (2018). Echocardiography and histology evaluation of the heart in the immature (2.5 years old) beluga. *Journal of Veterinary Research*, 72(4), 467–473. <https://doi.org/10.22059/jvr.2018.104369.2148>
- Zehtabvar, O., Vajhi, A. R., Tootian, Z., Rostami, A., & Shojaei, B. (2015). Computed tomographic anatomy and topography of the non-respiratory organs of coelomic cavity of European pond turtle (*Emys orbicularis*). *Jour-*

nal of Veterinary Research, 70(4), 411–418. <https://doi.org/10.22059/jvr.2016.56461>

How to cite this article: Zehtabvar, O., Masoudifard, M., Ekim, O., Ghorbani, F., Davudypoor, S., Memarian, I., & Zarghami Dastjerdi, P. (2022). Anatomical study of the scleral ring and eyeball of the Long-eared owl (*Asio otus*) with anatomical methods and diagnostic imaging techniques. *Veterinary Medicine and Science*, 8, 1735–1749. <https://doi.org/10.1002/vms3.823>